ASCI 2016 @ Boise

Characterization of Radiation Induced Microstructure in UO_2

Lingfeng He, Jian Gan

Idaho National Laboratory

May 18, 2016

www.inl.gov

Idaho National Laboratory

Irradiated microstructure and conductivity of UO_2

Conductivity degradation

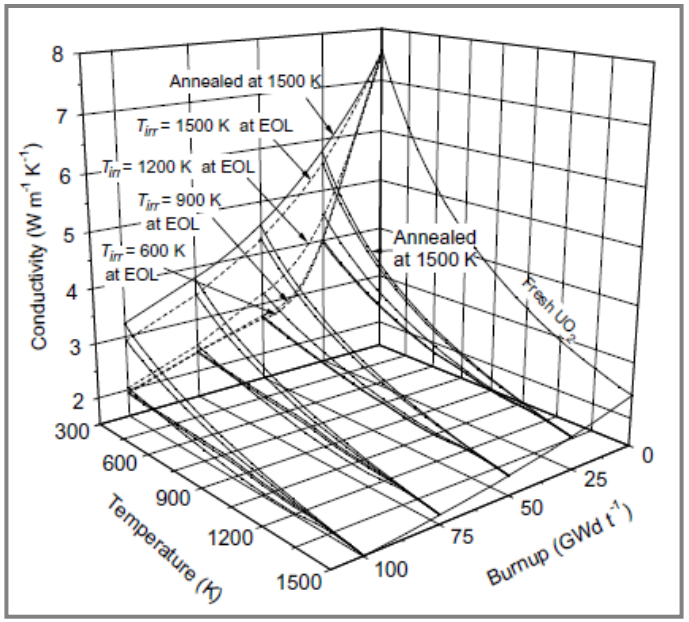

Ronchi et al, J. Nucl. Mater. 327 (2004) 58

Microstructure Complexity

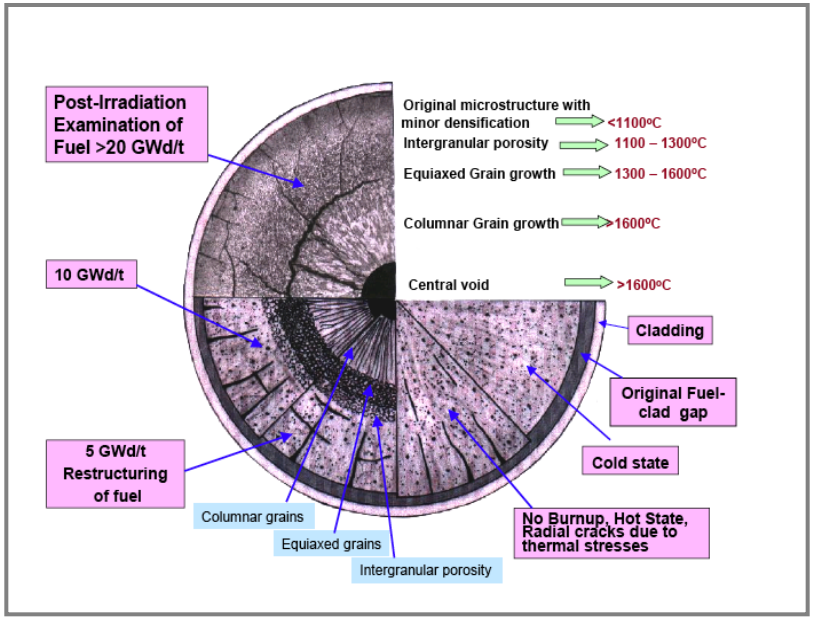

Graphic from S. Banerjee, Bhaba Atomic Research Center

Objective of microstructure study

To develop an experimentally validated multi-scale computational capability for the predictive understanding of the impact of ***microstructure*** on ***thermal transport*** in nuclear fuel under irradiation, with ultimate application to UO_2 as a model system.

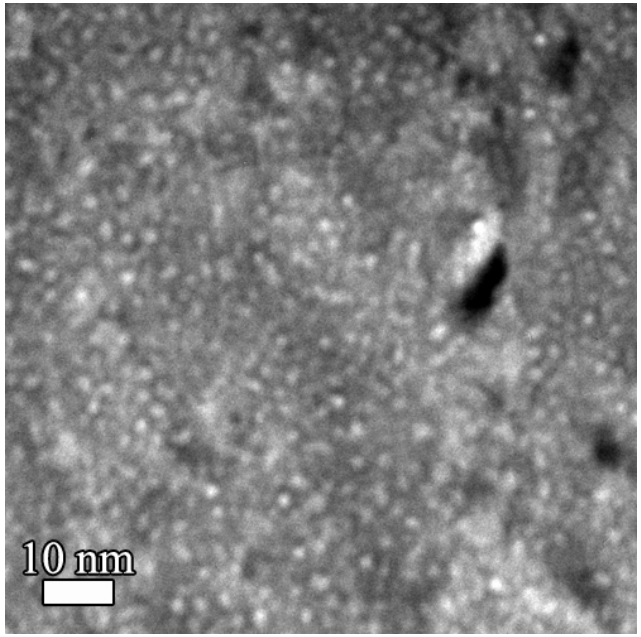

Kr bubbles

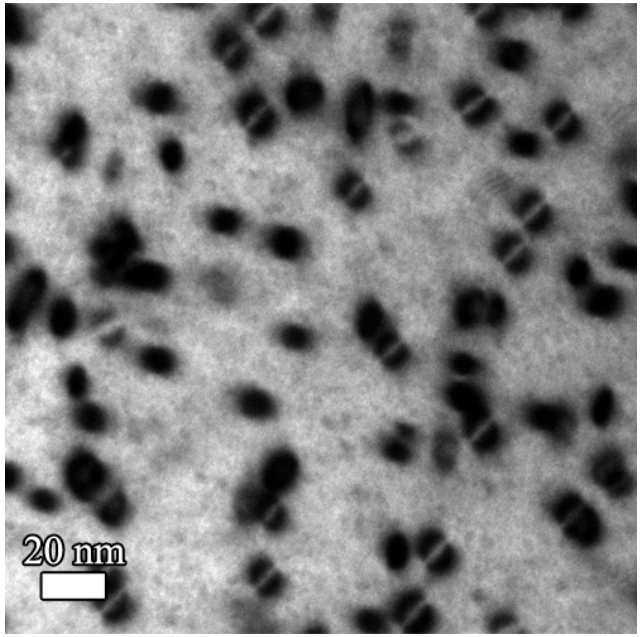

Discloation loops

In situ Kr and Xe irradiation at IVEM Tandem

- Kr and Xe are most common fission gas products in the reactor
- Implanted Kr and Xe in single crystal and polycrystalline UO_2 samples
- Ion energy and temperatures for irradiation

  150 keV & 1 MeV Kr

  300 keV Xe
- Dose from 1×10^{14} to 5×10^{16} ions/cm^2
- Temperatures are RT, 600°C, and 800°C
- Imaging for dislocation loops, dislocations, and bubbles
- Post-irradiation examination (FIB/APT/TEM/EDX/EELS)

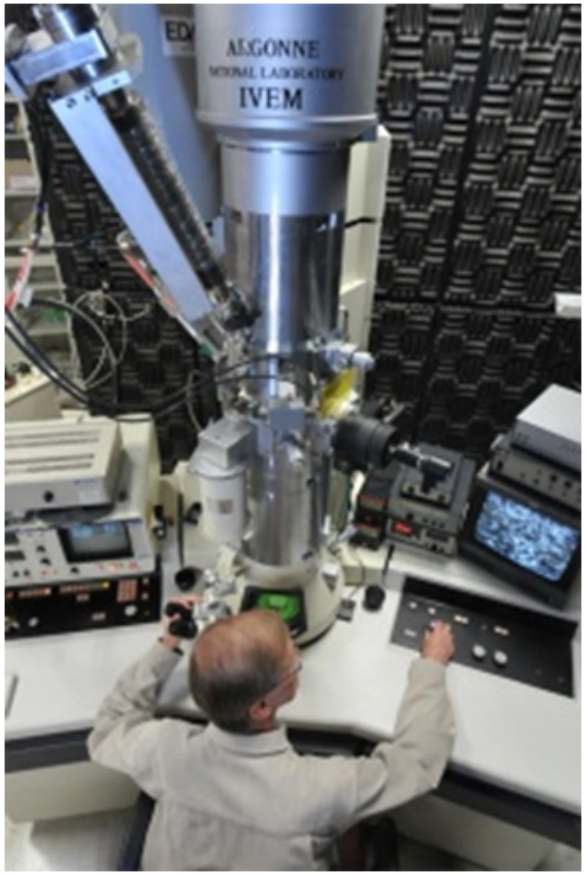

300 kV Hitachi 9000 NAR TEM (in situ)
300 kV Tecnai TF30-FEG STwin TEM (PIE)

In-situ dislocation evolution in UO_2 single crystal

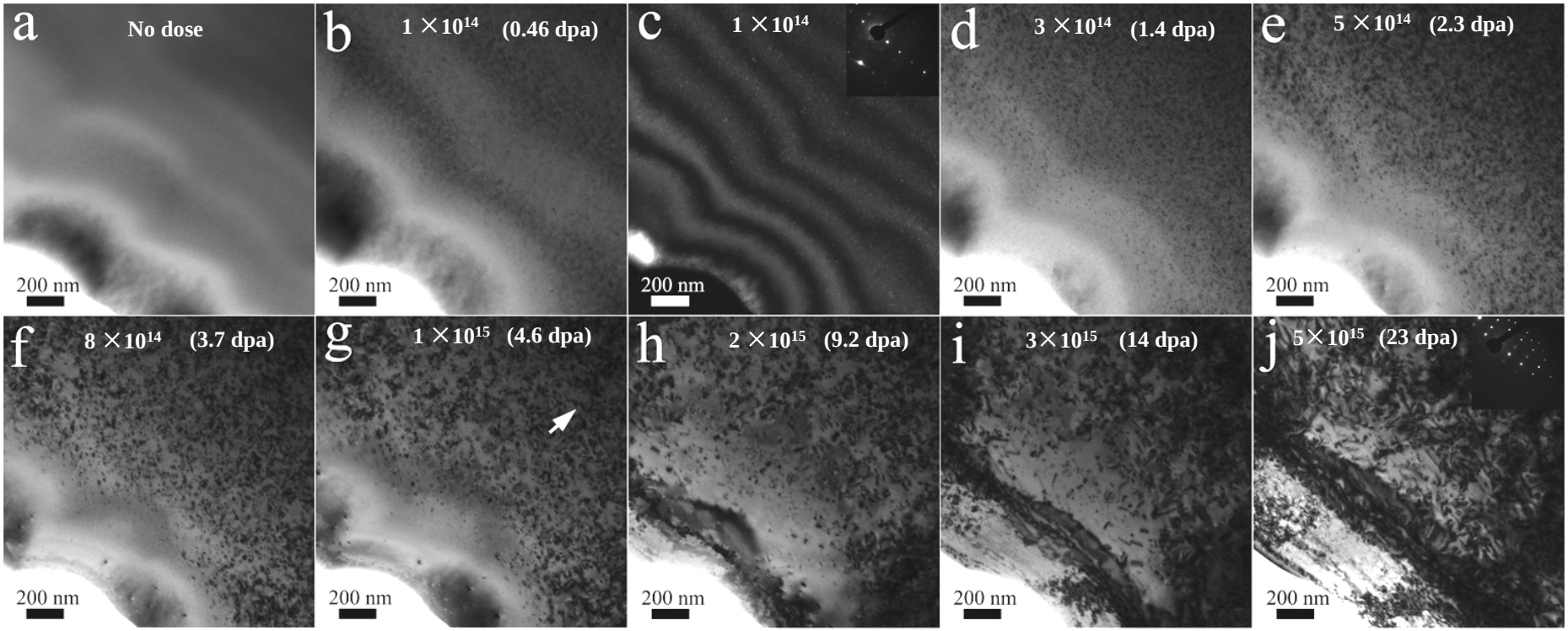

Dislocation loops grow quickly at low ion dose, transform to segments as dose increases, and finally transform to dislocation networks at higher doses through coalescence/coarsening mechanisms. There is a defect denuded zone near the edge of the foil.

1 MeV Kr @ 800 ^{o}C

L. He et al. J. Nucl. Mater., 443 (2013) 73

In-situ dislocation evolution in UO_2 single crystal

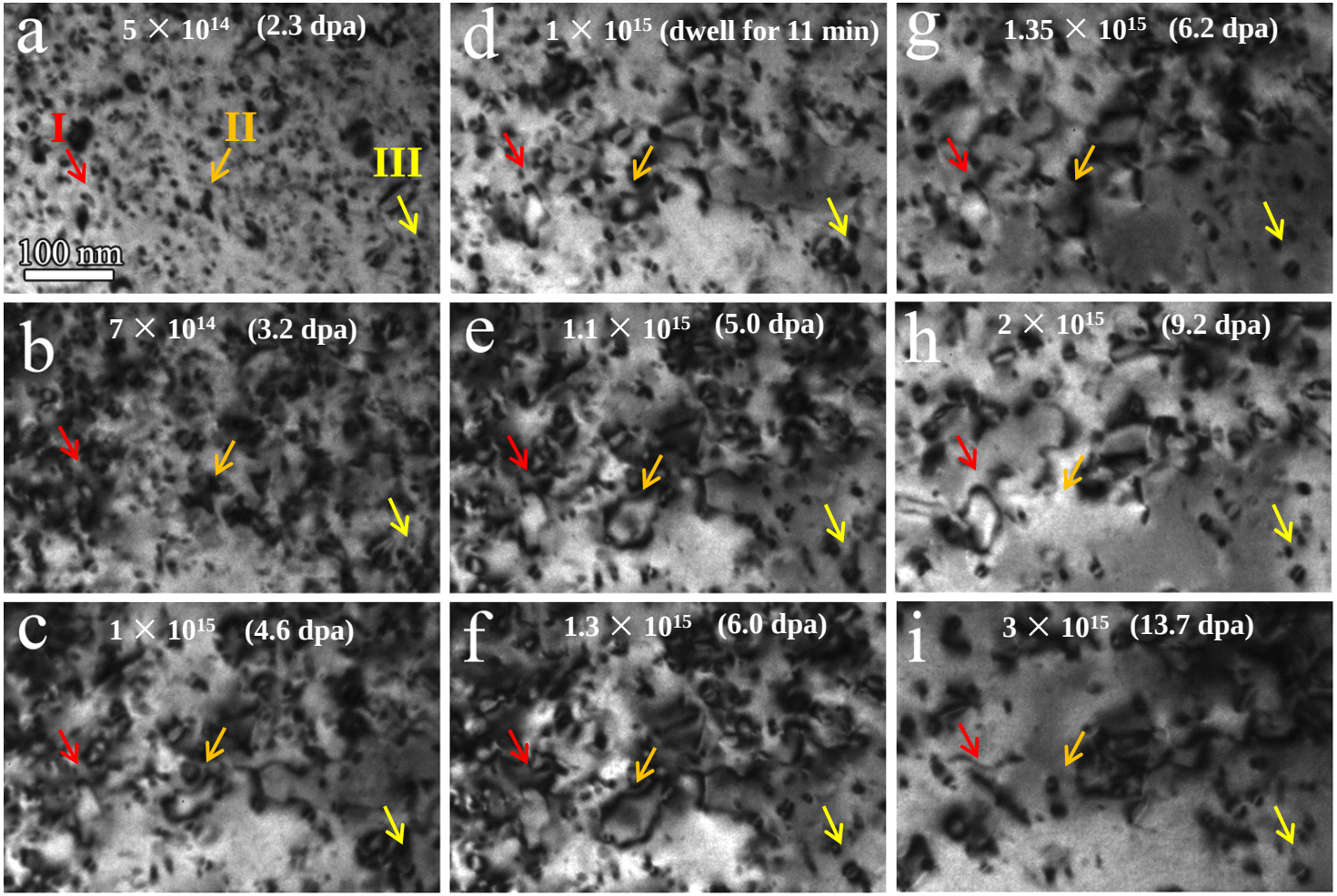

L. He et al. J. Nucl. Mater., 443 (2013) 73

Cross section of Kr-irradiated UO_2 single crystal

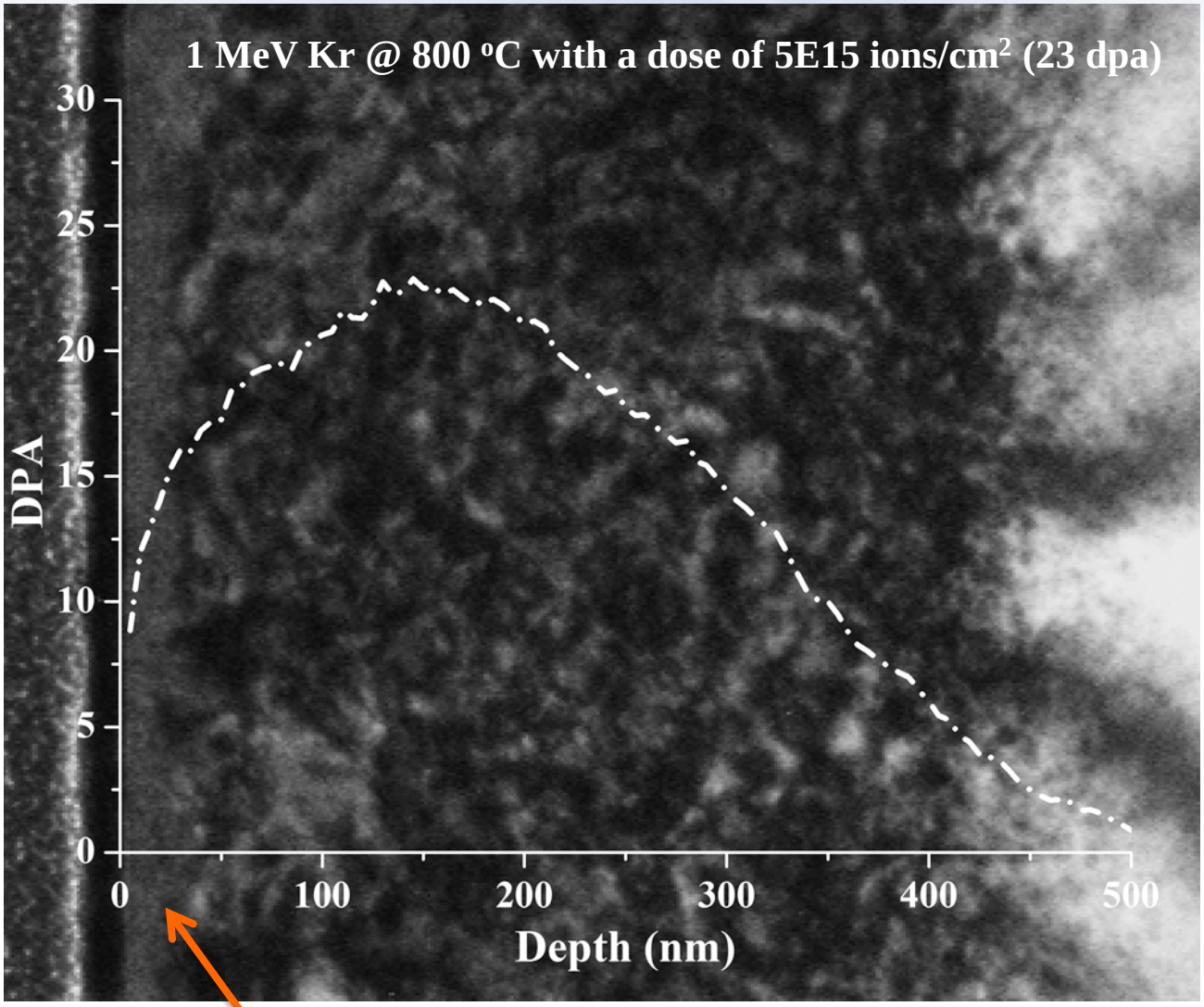

A dislocation denuded zone near surface

L. He et al. J. Nucl. Mater., 443 (2013) 73

Dislocation loop nature in Kr irradiated UO_2

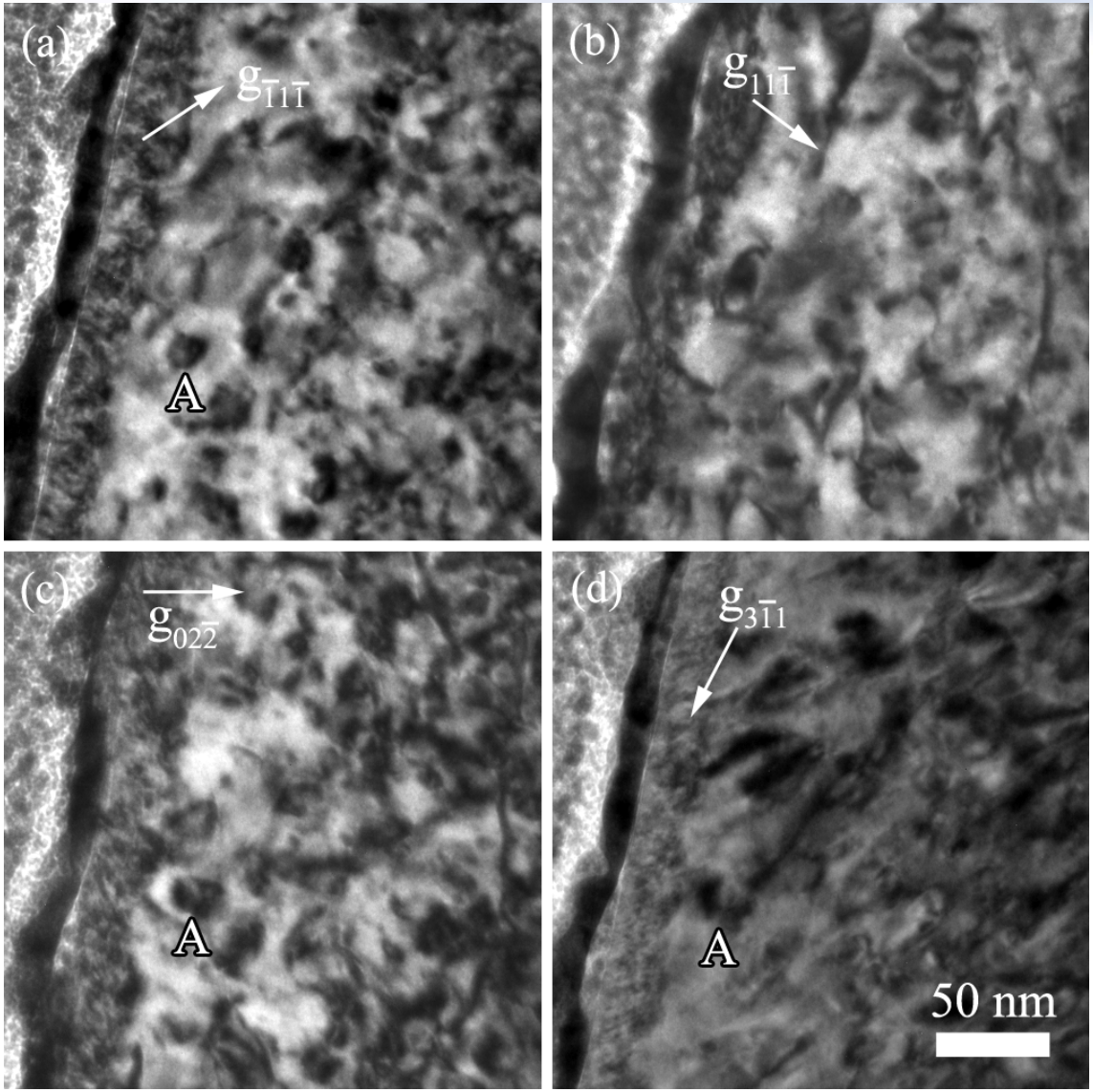

L. He et al. J. Nucl. Mater., 443 (2013) 73

$(g \cdot b)s<0$, inside contrast (I)

$(g \cdot b)s>0$, outside contrast (O)

$(g \cdot b)s=0$, invisible (X)

$(s>0)$

g	$[\bar{1}1\bar{1}]$	$[1 1\bar{1}]$	$[02\bar{2}]$	$[3\bar{1}1]$
loop	I	X	I	O

$b = ½<101>$

$B=z=[011]$

$b \cdot B > 0$

Loop A was determined as interstitial type with a burgers vector of ½<101>

In-situ dislocation evolution in polycrystalline UO_2

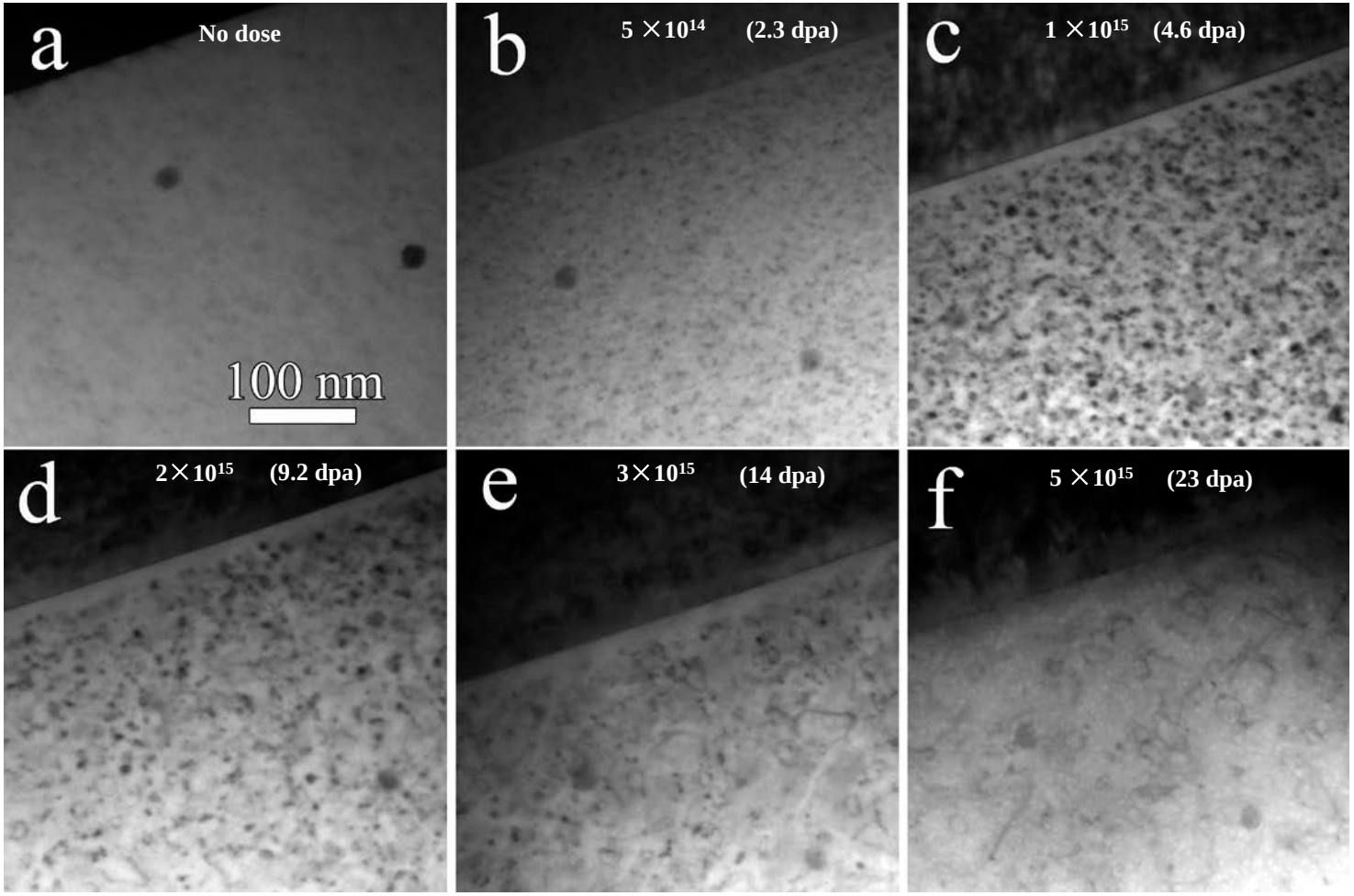

There is a defect denuded zone along the grain boundary in the whole dose range which will affect phonon scattering at the boundary.

1 MeV Kr @ 800 °C

L. He et al. JOM, 66 (2014) 2553

In-situ dislocation evolution in UO_2

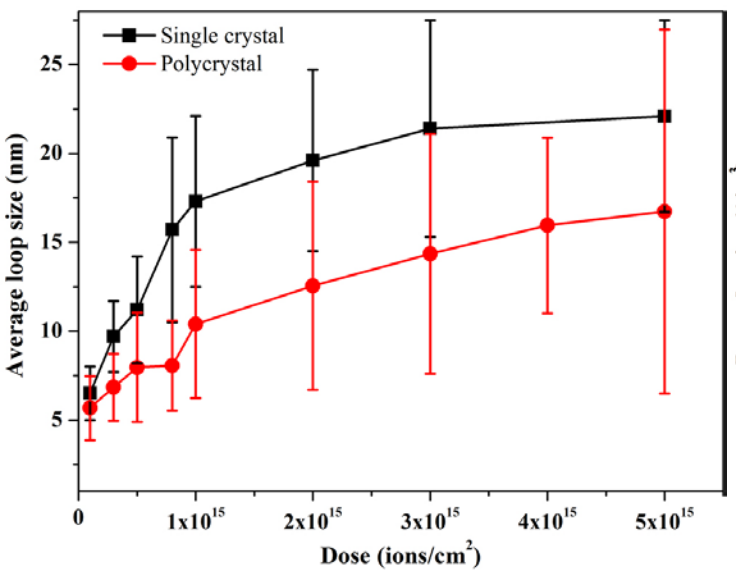

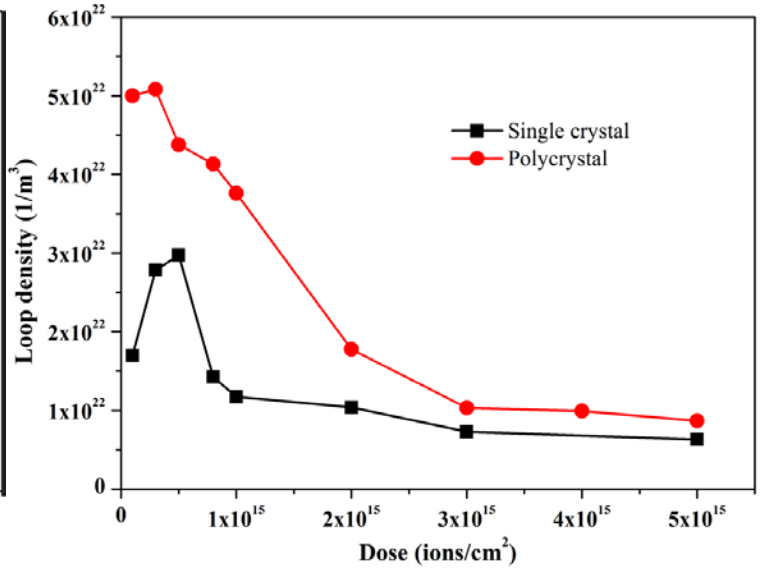

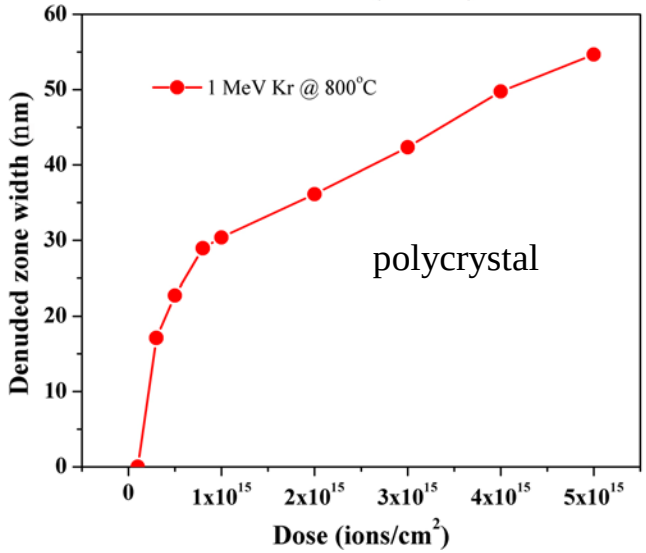

Dislocation loop size, loop density and denuded zone width in UO_2 as a function of dose

In-situ dislocation evolution in polycrystalline UO_2

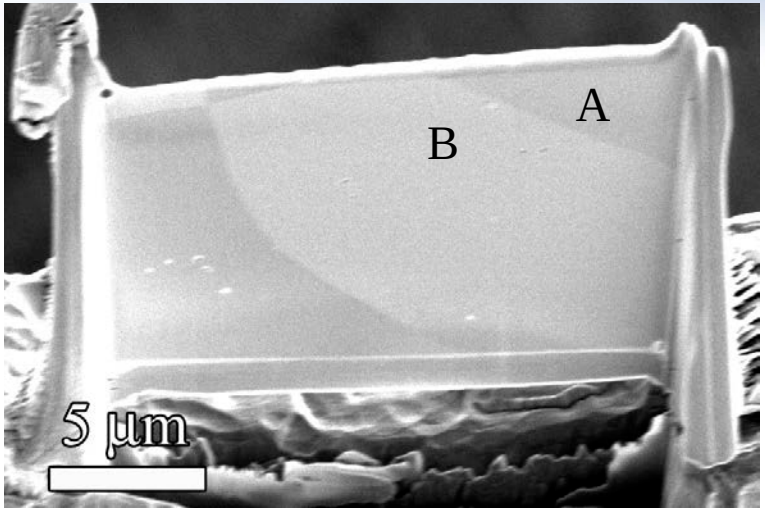

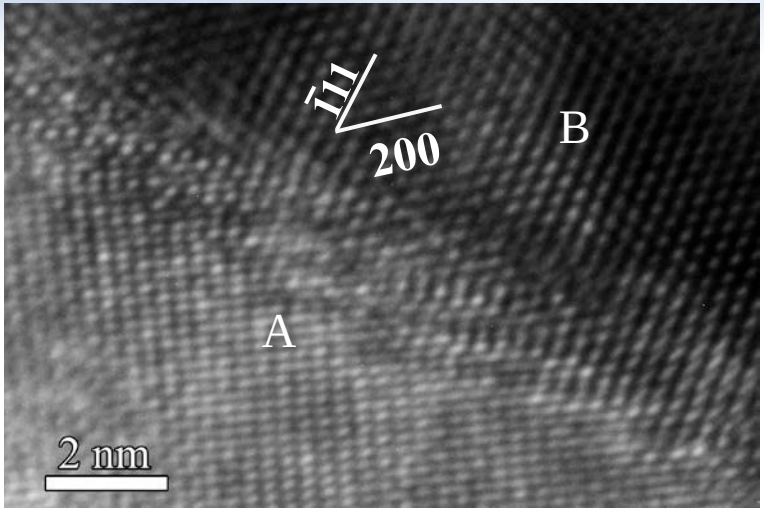

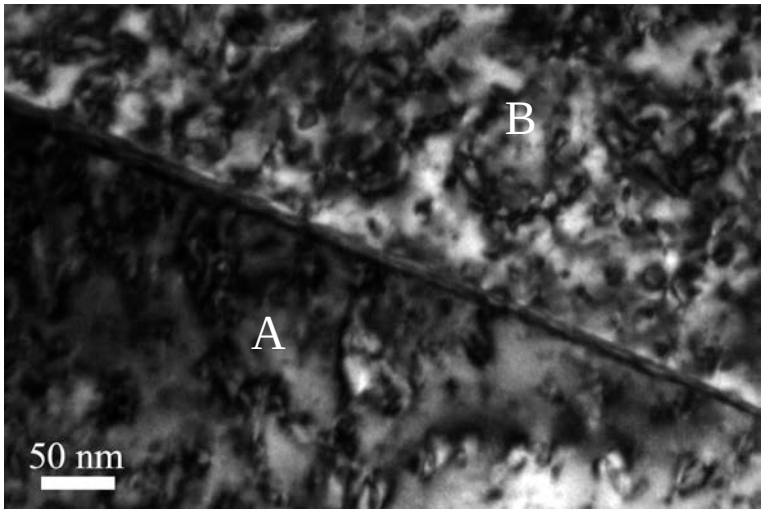

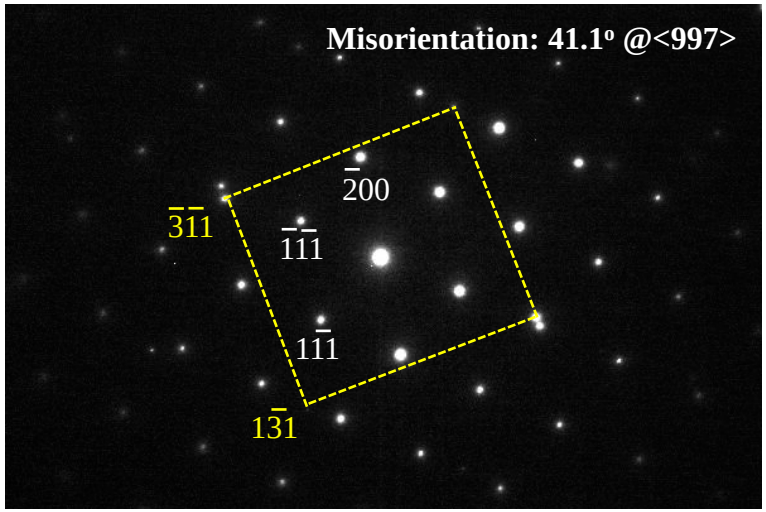

1 MeV Kr @ 600 °C with a dose of 5E14 ions/cm^2

No loop denuded

Grain A: z=[125]; grain B: z=[011]

L. He et al. JOM, 66 (2014) 2553

Summary of radiation induced dislocation loops

- Dislocation loops grow with ion dose, transform to dislocation segments and then tangled networks through coalescence/coarsening mechanisms. Interstitial-type dislocation loops with Burgers vector along <110> were indentified by the g·b analysis in the Kr-irradiated UO_2.

- Dislocation loop denuded zone along the grain boundary and near surface indicates that GB and surface act as good sinks for defects produced by Kr irradiation.

- The nucleation and growth of dislocation loops in UO_2 is more difficult than UN and U_2N_3, indicating higher radiation resistance of UO_2.

Kr distribution in UO_2

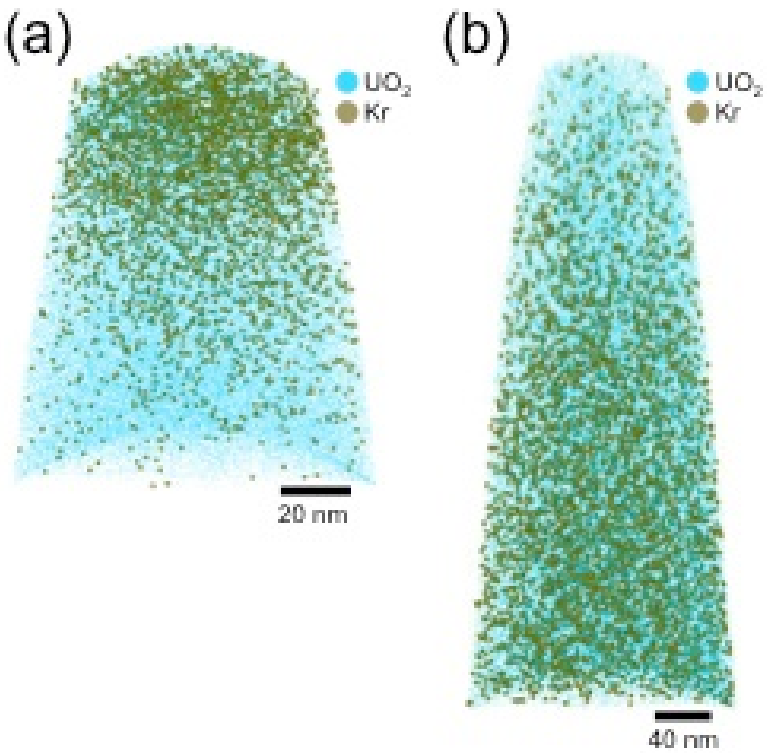

Atom probe tomography image of Kr in (a) 150 keV and (b) 1 MeV Kr-irradiated UO_2

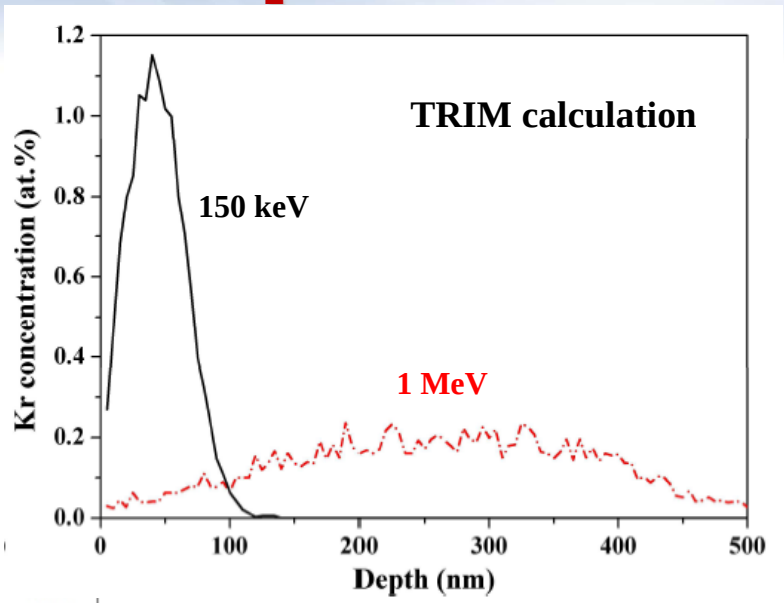

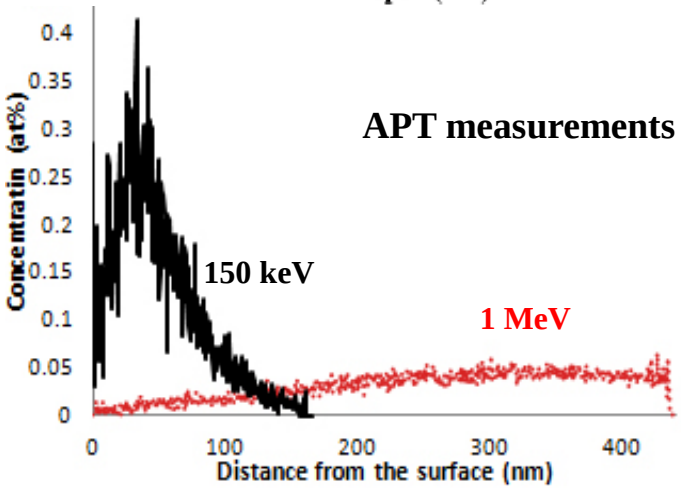

L. He & B. Valderrama et al. J. Nucl. Mater., 456 (2015) 125

Kr depth profiles in 150 keV Kr and 1 MeV Kr irradiated UO_2 at the dose of 5×10^{15} ions/cm^2

Kr bubble evolution in UO_2

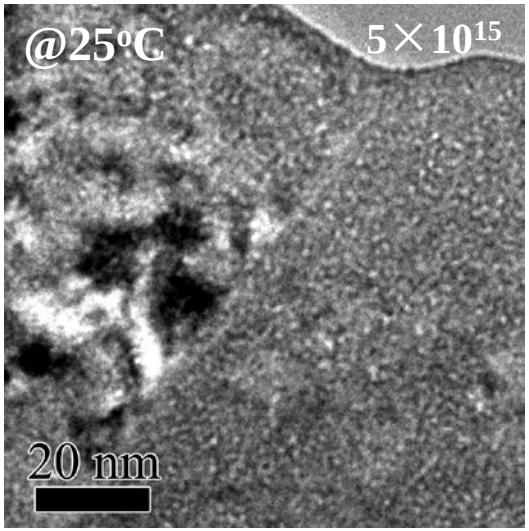

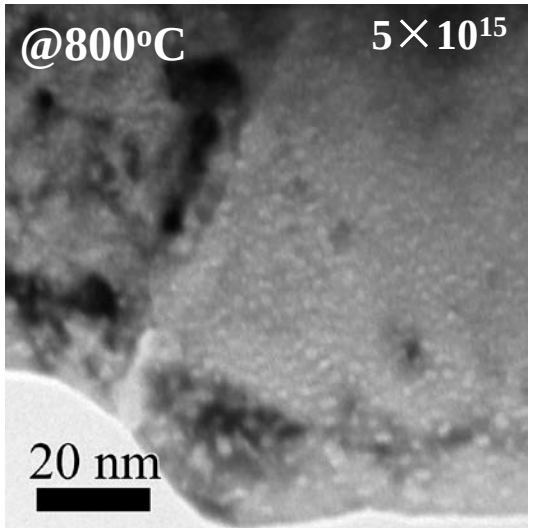

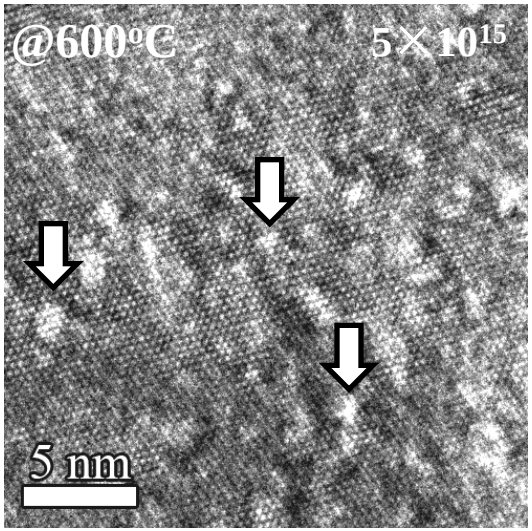

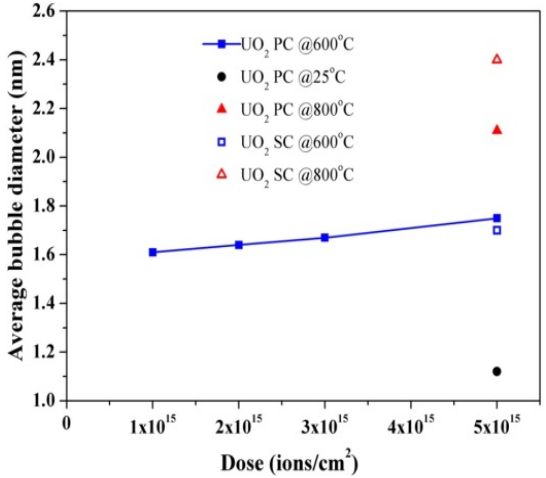

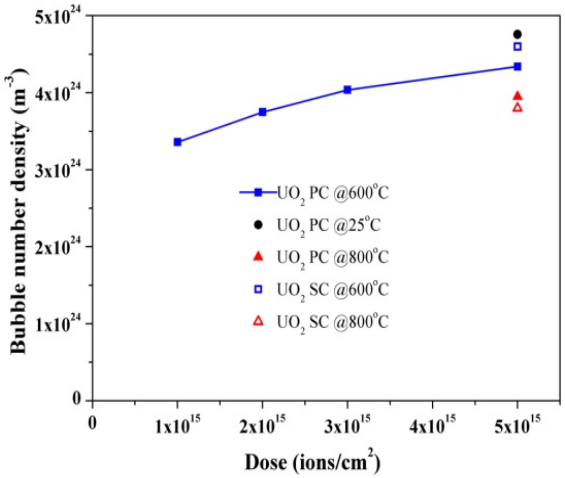

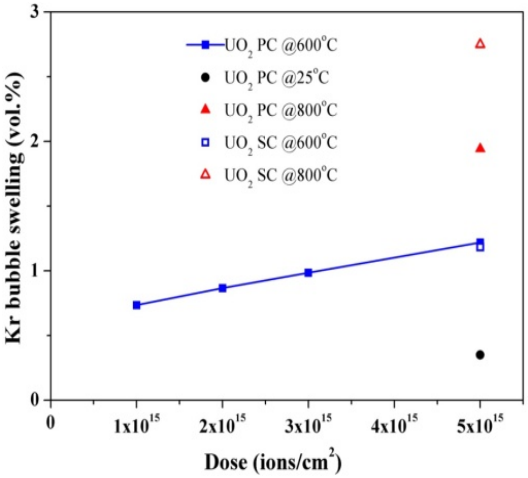

Dose dependence of bubble size, density and swelling in single crystal (SC) and polycrystalline (PC) UO_2 irradiated with 150 keV Kr at 25 and 600°C and 1 MeV Kr at 800°C

Stoichiometry of Kr irradiated UO_2

EELS spectra of Kr-UO_2

1 MeV Kr ions
@ 800 °C
5×10^{15} ions/cm^2

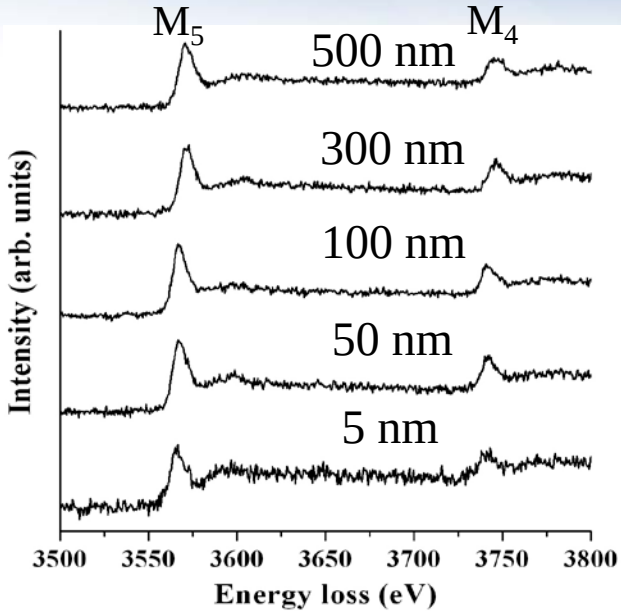

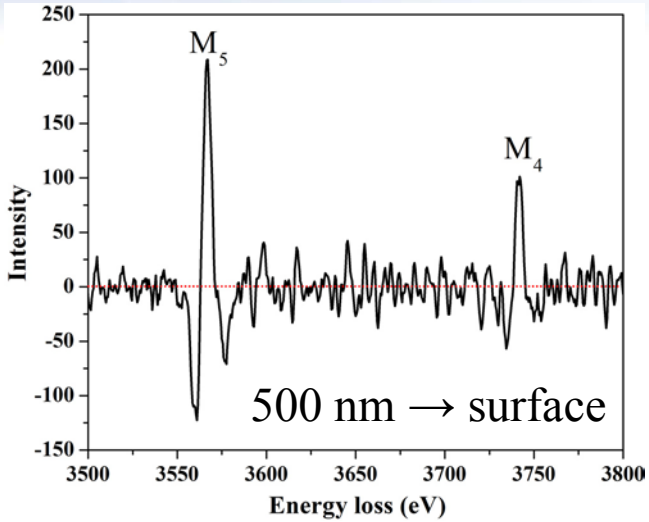

Second derivative of EELS spectrum

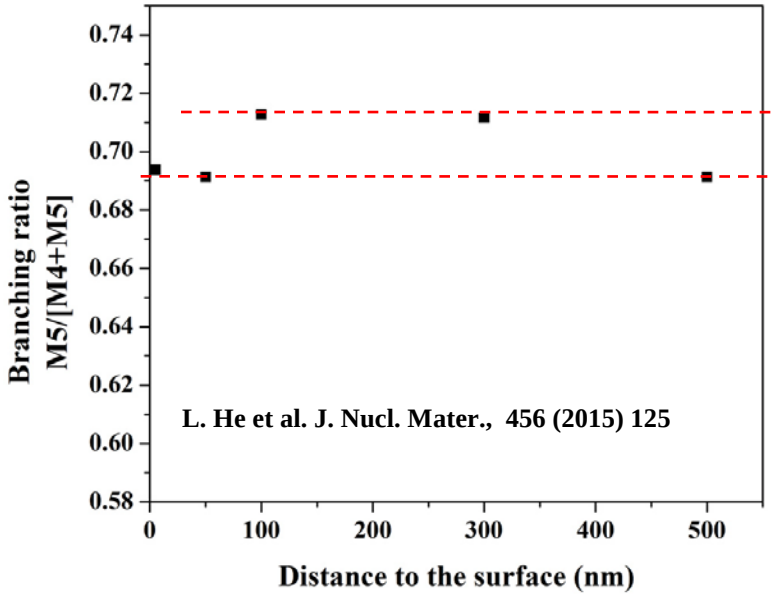

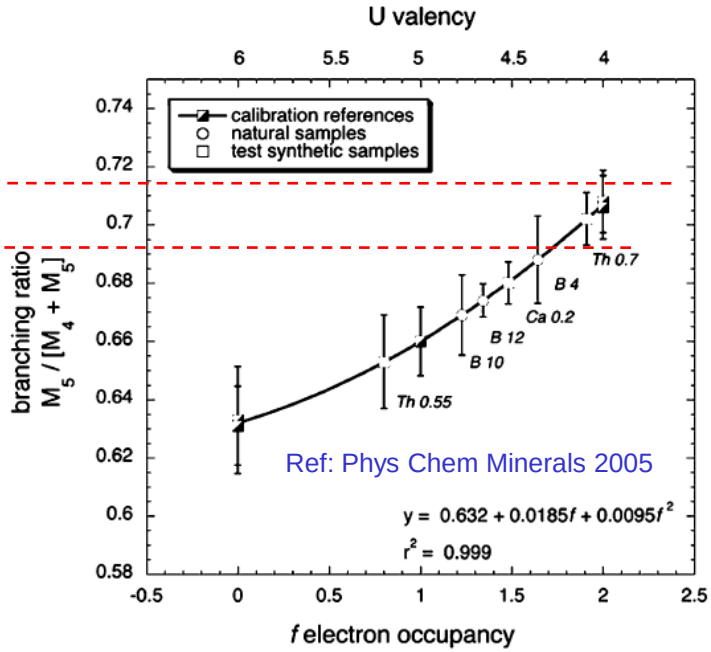

Summary of radiation induced bubbles

- Intragranular bubble size increases slightly and bubble density decreases slightly with increasing annealing temperature. Bubble distribution is in good agreement with the Kr depth profile calculated by SRIM.

Acknowledgements

This material is based upon work supported as part of the Center for Materials Science of Nuclear Fuel, an Energy Frontier Research Center funded by the U.S. Department of Energy, Office of Science, Office of Basic Energy Sciences, Laboratory Directed Research and Development (LDRD) program at Idaho National Laboratory as well as Nuclear Energy University Program, Office of Nuclear Energy.

Acknowledgements and collaborations

Janne Pakarinen, Mahima Gupta, Clarissa Yablinsky, Beata Tyburska-Pueschel and Todd R. Allen
University of Wisconsin – Madison

Marat Khafizov, David H. Hurley, Xian-Ming Bai, Jianguo Yu, Mitchell K. Meyer
Idaho National Laboratory

Billy Valderrama, Michele V. Manuel
University of Florida

Anter El-Azab
Purdue University

Marquis A. Kirk, Peter M. Baldo
Argonne National Laboratory

Brian Jaques, Darryl Butt
Boise State University

Andy Nelson
Los Alamos National Laboratory

Yaqiao Wu, Jatuporn Burns, Allyssa Bateman, Joanna Taylor, Kristi Moser-mcintyre
The Center for Advanced Energy Studies

Thank you for your attention!